Yan Hongru (Orcid ID: 0000-0001-7504-6802)
Huang Jianping (Orcid ID: 0000-0003-2845-797X)
He Yongli (Orcid ID: 0000-0002-0183-378X)
Liu Yuzhi (Orcid ID: 0000-0001-8310-6975)
Wang Tianhe (Orcid ID: 0000-0001-6475-263X)
Li Jiming (Orcid ID: 0000-0002-7286-3580)

Atmospheric Water Vapor Budget and its Long-Term Trend over the Tibetan Plateau

Hongru Yan[1], Jianping Huang[1*], Yongli He[1], Yuzhi Liu[1], Tianhe Wang[1] and Jiming Li[1]

[1]Key Laboratory for Semi-Arid Climate Change of the Ministry of Education, College of Atmospheric Sciences, Lanzhou University, Lanzhou 730000, China

Corresponding author: Jianping Huang (hjp@lzu.edu.cn)

Key Points:

- Despite air of Tibetan Plateau are moistening, atmospheric water supply is not able to alleviate the depletion of the surface water storage.
- Characteristics of water vapor balance vary across space in the Tibetan Plateau, with key areas including several basins.
- Regions around Yarlung Zangbo Grand Canyon suffer severe loss of water storage due to the overwhelming decrease in water vapor convergence.
- The surface water storage of the Three Rivers source region is also under risk of depletion.

This article has been accepted for publication and undergone full peer review but has not been through the copyediting, typesetting, pagination and proofreading process which may lead to differences between this version and the Version of Record. Please cite this article as doi: 10.1029/2020JD033297

Abstract

The rapid warming and consequent retreat of glaciers across the Tibetan Plateau (TP) has given rise to the debate on the ability of the atmospheric water supply to alleviate the depletion of surface water storage. We investigate long-term changes in atmospheric water vapor balance across the TP using 40-years ERA5 reanalysis. Precipitation, water vapor convergence and evaporation generally maintain an equilibrium but with different long-term variation trends: 0.68mm/a, -0.18mm/a and 0.69mm/a, respectively. Results suggest that the inability of the water vapor arriving from outside the TP to effectively replenish the surface water storage. Despit of huge changes in atmospheric water vapor balance during summer, the risk of water storage depletion are brought by other three seasons, especially the autumn. The climatology and long-term trends of water vapor balance exhibit strong variation across the regions of TP. The surrounding areas of Yarlung Zangbo Grand Canyon experiences sharp decrease in water vapor convergence, thus reducing precipitation. Moreover, increasing evaporation are expected to severely loss of surface water storage. For the Three Rivers Source Region with no significant changes in total precipitations, decrease in water transported from outsides of TP overlaps increase in evaporations results in the possible depletion of surface water storage. Brahmaputra basin, inner TP and Qilian Mountain exhibit significant wetting trends due to increases in both convergence of water vapor flux and evaporation. Above regional and seasonal characteristics of water vapor balances across the TP are attributed by inhomogeneous variation of atmospheric heat source and complex changes of atmospheric circulations.

Plain Language Summary

We aim to determine whether the increase in atmospheric water vapor is able to replenish the surface water storage depletion across the Tibetan Plateau (TP) by analyzing long-term trends in precipitation, water vapor convergence and evaporation. Results suggest that surface water storage will not be overall replenished by precipitation for the whole year, as despite the increase in water vapor from local evaporation, transportations from outside of the TP is reduced. Furthermore, long-term trends in the water vapor balance and their impacts on surface water storage vary from place to place across the TP.

1 Introduction

The Tibetan Plateau (TP), which has an area of 2.5 million km^2 and average elevation of over 4000 m, is the highest and most extensive plateau in the world. It serves as the "world water tower" storing large amounts of water as glaciers, lakes, and rivers (*Lu et al., 2005; Yao et al., 2012*). Seasonal melting of snowpack and mountain glaciers over the TP feeds seven major rivers in Asia, providing abundant fresh water to this region and its downstream areas, compromising approximately 40% of the world's population. Due to its unique terrain and specific underlying surfaces, the TP exerts a dramatic influence on regional and even global climate (*Wu et al., 2012a; Ma et al., 2017*). Therefore, investigating the atmospheric water over the TP is critical in climate research and adaptation policy.

Due to the Plateau "heat pump effect" (*Wu & Zhang, 1998*), the TP can attract water vapor from surrounding oceans or seas (*An et al., 2001; Boo & Kuang, 2010; Molnar et al., 1993; Wu et al., 2007, 2012b*), thus becoming an isolated region of humidity in the atmosphere (*Xu et al., 2008a*). The TP plays a significant role in adjusting the atmospheric circulation and hydrological cycle. Moreover, it is often considered as the "wet pool" and "transfer station" of the east Asian moisture during summer (*Wang et al. 2011*), exerting a great influence on the precipitation over downstream regions (*Wan et al. 2017; Xu et al. 2008b*) via the transportation of water vapor by the westerly winds and southwest monsoons (*Ding & Chan, 2005*).

Meanwhile, the TP snow cover associated with moisture anomaloy has a great impact on East Asian atmospheric circulation (*Li et al., 2018, 2019*). Therefore, TP is one of the most active global hydrological cycle centers, and thus understanding the water vapor transport from the TP and its subsequent impact on the regional weather and climate is crucial.

It was reported that TP is a climatologically moisture sink during summer, with a net moisture convergence of 4 mm/day (*Feng & Zhou, 2012*). On a diurnal scale, *Ueno et al*. (*2008*) determined a strong daytime wind speed accompanied by increasing relative humidity to prevail along deep valleys in the Himalayas. However, the weak southerly wind results in the stagnation of the water vapor in front of the Himalayas (*Ueno et al., 2008*). On the seasonal scale,, a synoptic trough is expected to have a strong impact on the water vapor transport from the Indian Ocean to the TP during the monsoon season (*Sugimoto et al., 2008*). In terms of a long-term trends, the precipitable water in the 680–310 hPa layer of the atmosphere has been reported toincrease significantly since the 1990s, with an upward trend of 6.45 cm per decade and 啊 particularly sharp rise during summer (*Zhang et al., 2013*).

The TP has experienced a rapid warming over the past 50 years, with warming rates reported to be double those of the global equivalent (*e.g. Liu & Chen, 2000; Guo & Wang, 2012*). Along with changes in the climate, atmospheric circulation and hydrological cycles are also altered and local environments are reshaped. The warming is accompanied by the moistening of air over the TP (*Xu et al., 2008a*), a significant increase in surface pressure (*Moore, 2012*), the weakening of surface and atmospheric heating (*Zhu et al., 2008; Duan & Wu, 2008, 2009; Yang et al., 2011a, 2011b*), and a decline in wind speed (*Lin et al., 2013*). Furthermore, the surface warming depends on elevation (*Liu & Chen, 2000*) and leads to glacier retreat, permafrost degradation (*Cheng & Wu, 2007*), lake expansion (*Zhu et al., 2010*), runoff increase (*Lutz et al., 2014*) and associated disaster risks aggravation (*Yao et al., 2012, 2019*). *Deng et al.* (*2018*) demonstrated an increase in the TP terrestrial water storage by 0.20 mm/month during 2002–2012, with a subsequent decrease of −0.68 mm/month since 2012. In addition, *Immerzeel et al.* (*2010*) projected that the warming may lead to less water resources for the downstream regions in the future.

The aforementioned observations and predictions from the previous research give rise to the following questions: How do each of the atmospheric water vapor budget components vary over the past 40 years across the TP? What factors are responsible for such long-term variations? Could the increasing in atmospheric water resources alleviate the depletion of terrestrial water storage caused by the melting of glaciers and the increase in runoff? Answering these questions can enhance our understanding of the long-term variability of water vapor budget over the TP in recent decades and the corresponding underlying mechanisms, and as well as allowing us to determine the significance of the atmospheric water tower in the hydrological cycle on regional and global scales.

In this study, we focus on the aforementioned questions in order to present a complete comprehensive understanding of the atmospheric water resources over the TP. In particular, we analyze the climatology of atmospheric water vapor over the TP based on ERA5 reanalysis data. We then examine the climatology and long-term variations of each component of the water vapor budget (water vapor transportation, evaporation and precipitation). Finally, we discuss the atmospheric water balance over the TP. The rest of the paper is organized as follows. Section 2 describes the data and accuracy of each parameters, as well as all methods and formulas used in this study. Section 3 presents and discusses the results and and Section 4 concludes the atmospheric water budget and its long-term trends over the TP.

2 Data and Methods

2.1 Dataset

ERA5 is the fifth generation European Centre for Medium-Range Weather Forecasts (ECMWF) atmospheric reanalysis for the global climate and weather for the past 4 to 7 decades, which is a replacement of ERA-Interim reanalysis. It has published a detailed record of the evolution of the global atmosphere from 1979 to update and will be from 1950 onwards when complete (*Berrisford et al., 2009; Dee et al., 2011*). Based on the 4D-Var assimilation method, ERA5 provides hourly global estimates. The native resolution of the ERA5 atmosphere and land reanalysis is 31km on a reduced Gaussian grid (Tl639) and 63km (TL319) for the ensemble members. The atmospheric component consists of 137 vertical levels from the surface up to 1 Pa (approximately 80 km), spanning the troposphere, stratosphere and mesosphere. Data has been regridded to a regular lat-lon grid of 0.25 degrees for the reanalysis. The dataset consists of two principle subsets: pressure level and single level data. The former contains 16 atmospheric quantities on 37 pressure levels from 1000 hPa (surface) to 1 hPa (around the top of the stratosphere), while the latter is available for a number of atmospheric, ocean-wave and land surface quantities. Information on the current status of the ERA5 production, availability of data online, and near-real-time updates of various climate indicators derived from ERA5 data, can be found at http://www.ecmwf.int/research/era. We employed following parameters from ERA5 monthly datasets to investigate the atmospheric water tower over the TP: total column water, specific humidity, vertical integral water vapor flux, vertical integral moisture divergence, evaporation, snow evaporation and precipitation.

Caution must be applied when using reanalysis dataset to investigate trends in water vapor, precipitation and evaporation due to their qualities over the TP. *Wang et al.* (*2017*) and *Zhao and Zhou* (*2019*) demonstrated that total column water vapor from ERA5 performance well over TP. In the current study, we evaluate the quality of evaporation and precipitation in ERA5 datasets via comparisons with the satellite retrievals and other reanalysis datasets. In particular, we compare the ERA5 evaporation with the relatively accurate evaporation data developed by *Chen et al.* (*2019*), which revised the Surface Energy Balance System (SEBS) parameterization of bare soil to correct the biases of excess resistance to heat transfer. This satellite-based product has been demonstrated to perform well. The 2001-2016 ERA5 monthly mean evaporation is highly correlated with the satellite observations, with a correlation coefficient of 0.84 and mean absolute deviation of 13.0 mm (Figures S2). Furthermore, we also compared the precipitation from ERA5, ERA-interim, the Global Precipitation Climatology Project (GPCP v. 2.3, *Adler et al., 2003*), and the Climatic Research Unit (CRU, TS v. 4.03, *Harris et al., 2020*) with that from the High Asia Reanalysis (HAR, *Maussion et al., 2014*), which is recognized good performance over the TP (*Li et al., 2020*). Among those datasets, the ERA5 monthly precipitation exhibited the lowest bias of -5.4 mm and highest correlation coefficient of 0.97 (Figures S1).

2.2 Methods

2.2.1 Atmospheric Water Resources over the TP

We employ specific humidity vertically integrated from 500 hPa to 300hPa to represent the atmospheric water resources over the TP. This allows for the investigation of atmospheric water resources over the TP. The vertically integrated specific humidity (kg/m^2, equivalent to mm) is determined as follows:

$$w = -\frac{1}{g}\int_{500}^{1} q\, dp,$$

where g is gravitational acceleration of 9.8 m s^{-1}, q is the specific humidity (kg kg^{-1}), p is pressure level (Pa). Figure 1 indicates that the altitudes over the TP are greater than 4000km.The climatological surface pressure over the TP ranges from 500 hPa to 700 hPa, while the water vapor is generally concentrated in the lower troposphere, thus we intergrated the water vapor between 500 hPa to 300 hPa (Wang et al., 2009; Zhou et al. 2013).

2.2.2 Atmospheric Water Balance over the TP

The atmospheric water vapor budget equation (*Chou & Neelin, 2004; Zhou et al., 2019*) is expressed as:

$$\frac{\partial w}{\partial t} = -\nabla \cdot Q + E - P + res \quad (1)$$

where w is vertically integrated atmospheric water vapor, P and E are precipitation and evaporation, respectively. $\frac{\partial w}{\partial t}$ is the time derivative of the vertically integrated moisture, $-\nabla \cdot Q$ is the horizontal divergence of water vapor and *res* is a residual term, which is possible related to the assimilation in the reanalysis dataset. Note that although $\frac{\partial w}{\partial t}$ is much smaller than other terms in Eq.(1), and is typically neglected, it also determines the atmospheric water vapor trends over the TP. In order to investigate the mechanism underlying the long-term variation of atmospheric water tower over the TP under global warming, we individually examine the horizontal net water vapor flux, evaporation and precipitation (Section 3.2).

2.2.3 Horizontal Net Water Vapor Flux over the TP

Based on Green's theorem (sum of fluid outflowing from a volume is equal to the total outflow summed about an enclosing area), we use following two independent methods (Equation (5) and (6)) to compute the horizontal net water vapor flux over the TP.

$$IQU = \int_{sfc}^{toa} \frac{qu}{g} dp \quad (2)$$

$$IQV = \int_{sfc}^{toa} \frac{qv}{g} dp \quad (3)$$

$$D = \frac{\partial IQU}{\partial x} + \frac{\partial IQV}{\partial y} \quad (4)$$

$$N = \oint_{tp} IQU dy + IQV dx \quad (5)$$

$$N = \oiint_{tp} D \, d\sigma \quad (6)$$

where q is specific humidity, u and v are eastward and northward wind speeds, respectively; *IQU* and *IQV* are the eastward and northward water vapor fluxes, respectively; D is vertical integrated water vapor flux divergence, where positive values indicate the moisture spreading out and negative values indicate moisture concentrating or converging; σ is the area of grid (km^2); and N is the net income of the atmospheric water resource for the entire TP area (Gt).

3 Results

3.1 Climatology/Feature of Atmospheric Water Tower

Figure 2 presents the zonal deviation of the annual mean vertically integral specific humidity The long-term annual mean and seasonal means of vertically integral specific humidity above 500 hPa over the TP can generally be considered as wet in southern and

southeastern TP and dry in northwestern and northeastern TP. The peak moisture is located above southern TP and south of the Himalayan region in the middle and upper stratosphere. This long-term wet pool in the high atmospheric layer indicates an atmospheric water tower (AWT). The formation of this AWT is attributed to the elevated terrain of the TP, which acts as a heat source and pumps water vapor from the low-levels of the Arabian Sea and Indian Ocean to the high-levels of TP. Higher altitudes facilitate the transport of water vapor across larger distances and present a ‘‘re-channel function’’ at the planetary-scale (*Xu et al., 2008a*). The Yarlung Zangbo Grand Canyon and the relatively lower elevation in southeastern TP allow the warm and humid airflow from the oceans or seas to travel up the south slope of the TP and enter the inner land. Furthermore, the polar dry air is blocked on the north side of the TP, while the water vapor from the south cannot be easily transported to the north. These processes lead to the extreme dry climate in the north side of the TP. Central location exhibit significant annual variation in the maximum moisture. In winter, the wettest center is located in the southeast of TP, with a vertically integral specific humidity peak value less than 1 kg/m^2. As spring approaches, the maximum center spreads to the north and west, with the peak value reaching 3 kg/m^2. In summer, wet regions occupy the entire southern TP region, with a maximum value close to 7 kg/m^2. These wet regions subsequently shrink back to the southeast of the TP with the arrival of autumn. This annual variation indicates that the strong influence of the South and East Asian monsoons on atmospheric water resource over the TP. In particular, wet areas expand and moisture in atmosphere increases with the outbreak of the summer Asian monsoon.

Over the past few decades, the increase rate of air temperature in the TP is almost two times higher than that in the global (*Chen et al., 2014*). This enhanced rate may have accelerated the melting of glaciers and snow. As atmospheric water resource are key for the supply of surface water resources, long-term trends of atmospheric water resources over the TP are of interest. Figure 3 depicts the horizontal distribution of the long-term trends for vertically integral specific humidity above 500 hPa over the TP. From 1979 to 2018, the atmospheric water resources across the main body of the TP exhibit significant growth trends, with the exception of the wettest region in southeastern TP. The distribution trend during summer agrees with the overall long-term trends, yet the values are larger for the former. The remaining three seasons exhibit increasing long-term trends that are consistently smaller than that of summer. This upward trends may be a result of the variations in atmospheric circulation and heat sources during summer. The inner TP, where conditions are relatively dry, is observed as the wettest region, while the southeastern TP, the wettest climate, become slightly dryer. *Xu and Gao* (*2019*) associates the decreasing trends in southeastern TP with the lower water vapor transportation from the Indian Ocean.

3.2 Atmospheric Water Balance over TP

Previous researches has attributed the variations in water vapor over TP to multiple factors, including atmospheric circulation, temperature, elevation and land surface process (*e.g., Duan et al., 2018; Zhou et al., 2019; Xu & Gao, 2019*). Thus, we analyze the water vapor budget to investigate long-term trends in water vapor convergence, evaporation and precipitation across the TP (Figure 6), following previous studies (*Chou & Neelin, 2004; Zhou et al., 2019*). We calculate the moisture budget equation using Equation (1).

3.2.1 Horizontal Net Water Vapor Flux over the TP

Figure 4 presents the vertical integral of the water vapor flux within the four boundaries over the TP determined using Equation (5) and the ERA dataset for 1979-2018.The results demonstrate that the water vapor over the TP was transported from the western and southern boundaries with water vapor flux of 1328 Gt /a and 2195 Gt /a, respectively. The water vapor

then flows out of the eastern and northern boundaries with fluxes of -2225 Gt /a and -252 Gt /a, respectively. This is consistent with previous study based on ERA-Interim (*Zhou et al., 2019*). Therefore, the atmospheric water tower is mainly influenced by the water vapor transported from the west and south of the TP, which is associated with the interaction between westerly and monsoon system (*Yao et al., 2019*). *Xu et al*. (*2002, 2019*) presented a conceptual model of the key influence area of water vapor transport, denoted as the "large triangle sector", in the TP and low-latitude ocean monsoon region. This model considers the TP as a transfer station drawing water vapor from the Indian Ocean and transfers it downstream. The transport of water vapor into the TP results in 1046 Gt of water vapor left to form precipitation or increase atmospheric water vapor content annually.

Figure 5 presents the long-term trends in the net water vapor flux over the TP region and accumulated water vapor flux passing through four boundaries. A slight increase is observed for the annual mean of net water vapor flux over the TP by 1.9 Gt/a, which is dominated by the summer trend. The increasing trend of atmospheric water tower is induced by the enhanced inflow transportation from the western boundaries and the decreasing outflow transportation in the eastern boundary. However, the reduction in the inflow transportation from southern boundary and the increasing outflow transportation from northern boundary weaken the increasing trend in the net water vapor flux over the TP. Analysis of the seasonal transportation within four boundaries reveals the significant increase in the net water flux over the TP during summer, while values decrease slightly in autumn and winter. Furthermore, there is a dramatic change in the water vapor flux trend in summer, with limited variations during the three remaining seasons. Although the west and south boundaries are considered as water vapor channels in the climatology, the water flux trends in these boundaries do not exceed those of eastern and northern boundaries, especially during summer. The rise in the net water vapor flux over TP may be not induced by the interaction between the westerly and monsoon systems. The summer water vapor flux of the northern boundary and the annual mean both exhibit significant decrease. This may be attributed to the northward shift of subtropical westerly jet (*Lin et al., 2013*) and cyclonic anomalous near Lake Baikal (*Zhou et al., 2019*). The decreasing of water flux in the eastern boundary makes the greatest contribution to the net water vapor flux trend and may be associated with the weakening of wind speed over the TP (*Lin et al., 2013*).

Figure 6 depicts the long-term annual and seasonal mean distribution of divergence of vertically integrated water vapor flux (*D*) over the TP based on Equation (4). The water vapor flux is observed to converge across the majority of the TP, with the expection of several locations in northwestern TP. In particular, a weak convergence (less than 100 mm annually) is demonstrated for western and northern TP, with stronger convergences (up to 4000 mm annually) in the south slope and southeast of the TP. The highest converging center, which is along with Yarlung Zangbo Grand Canyon, has been recognized as the major entrance passageway for water vapor into the TP (*Xu et al., 2002*). The distribution of the water vapor flux divergence exhibits significant seasonal variation. For example, the winter converging center of water vapor flux is located in Nyingchi, with a maximum value of approximately 300 mm, while the rest of the surrounding area exhibits a diverging trend. In spring and autumn, the converging center expanded to the southeast of the TP. The approach of summer is associated with the convergence of water vapor for almost the entire TP and almost half of the TP exhibits a diverging water vapor flux exceeding 300 mm. This seasonal variation highlights the strong impact of the South Asian monsoon and East Asian monsoon as well as the topography of the TP on the transportation of the atmospheric water vapor. The net income of the atmospheric water vapor for the entire TP via Equation (6) is determined as 1103.6 Gt, which is close to that (1046 Gt) calculated by Equation (5).

The divergence of the vertically integrated water vapor flux decreases dramatically at the highest converging center located at the Yarlung Zangbo Grand Canyon, while more moderate reductions observed for the Qaidam Basin and the east of the TP. Areas associated with weak convergence (e.g., the Qilian Mountain and the inner TP) exhibit long-term upward trends in the divergence of water vapor flux (Figure 7). The long-term decreasing trend at the Yarlung Zangbo Grand Canyon is consistent across seasons. Furthermore, similarities are observed for the distribution of long-term water vapor divergence trend between summer and the annual mean, with much larger trends compared to other seasons. *Duan et al.* (*2018*) identified a weakening trend in the heat of the TP based on site observations since the 1980s, while the reverse was true in *Luo et al.* (*2019*) for plateau heat sources based on reanalysis data. The observation sites are mainly distributed in the southeast of the plateau, with a severe lack of the sites in the middle and northwest of the plateau. This may explain the disagreement between heat source data from the observations and the reanalysis data. Therefore, the long-term trends in divergence of water vapor flux and heat sources demonstrate similar patterns, namely, the southeast region exhibits a cooling and drying trend, while the central and northwestern parts show a warming and wet tendency. This reveals the dominant influence of atmospheric heat sources on moisture convergence. *Ma et al.* (*2017*) attribute the weakening water vapor transportation in the southeast of TP is due to wind stilling. Lower water vapor transportation from the Indian Ocean might be another reason to the decrease trend observed for southeastern TP (*Xu & Gao, 2019*). However, a greater atmospheric water content may absorb a larger amount of long-wave radiation and intensify the apparent heating source, which could strengthen the convergence of water vapor, thus forming a positive feedback. In addition, *Yang et al.* (*2011b*) point out the water vapor increasing might lead to solar diming over the TP. Thus, the feedback resulting from increasing water vapor to the heat source requires further clarification.

3.2.2 Evaporation over the TP

In order to estimate the total evaporation over the TP, we sum the evaporation and snow evaporation obtained from ERA5 (Figure 8). Annual accumulated total evaporations are up to 800 mm/a in southeast of TP but drop to 100 mm/a in the west and northwest regions. The evaporations ranges are observed to strongly agree with the divergence of water vapor flux across the majority of the TP. As most of the lakes in the TP scattered over the inner TP, evaporation is relatively higher in this region. The lowest evaporation (< 100 mm/a) is located at the Qaidam Basin, which is also the driest area of the TP. The locations of maximum and minimum evaporation are consistent across seasons, while the total evaporation exhibits significant seasonal variations in magnitude due to the changes of air temperature. For example, during summer, areas with evaporation over 200 mm compromise approximately 80% of the TP, while the evaporation values for spring and summer are about two thirds of that in summer and double that in winter.

The total evaporation generally exhibits a significant increasing trends over the TP, with the exception of a few of places, including the Qaidam Basin and Karakorum Mountains (Figure 9). This generally agrees with an the independent modeling study (*Yin et al., 2013*) and site observations (*Zhang et al., 2007; Yang et al., 2014*). The TP has experienced enhanced temperature increase, glaciers melting and lake expansion over the past few decades (*Yao et al., 2019*), hence an increase in evaporation expected. Regions exhibiting increasing evaporation can be divided into two categories based on the observed seasonal variation. The first category is located in the western and inner TP, and demonstrates significant seasonal variation with a notable increase during summer and autumn, a slightly increase in spring and a reduction in winter. The second category is located in the southeastern TP, where

evaporations increases consistently during the entire year with limited small seasonal variations. Impacts on actual evaporation includes the surface water availability, the temperature gradient between the air and surface and wind speed. The latter two factors dominate the evaporation in wet areas, and thus an increase in evaporation in the southeast of the TP is generally attributed to a rise in air temperature. However, the elevated evaporation in the western and inner TP is the result of an increases in both temperature and water availability at the surface. Based on the Gravity Recovery and Climate Experiment (GRACE), *Deng et al.* (*2018*) found a reduction in terrestrial water storages in the southern TP , with the reverse true for the Inner TP from 2002 to 2016. Moreover, *Wan et al.* (*2016*) employed ground surveying and high-spatial-resolution satellite images to establish a lake data set from 2004 to 2015 for the TP, identifying and an increase in the lake area and a decrease in the Brahmaputra basin. This suggests that a consistent trend between the evaporation and water availability at the surface.

3.2.3 Precipitation over the TP

Water vapor flux divergence and total evaporation form atmospheric water vapor resources and result in precipitation. Figure 10 presents the horizontal distribution of the 40-year (1979-2018) annual accumulated total precipitation (Figure 10). The precipitation distribution integrates characteristics from both the divergence of water vapor flux and evaporation. The maximum precipitation (>1500 mm/a) coincides with the largest converging center and is located close to the Yarlung Zangbo Grand Canyon. The minimum precipitation (< 150 mm/a) is observed in the Qaidam Basin, which is also the location of the lowest evaporation. The relatively low water vapor convergences (approximately 300 mm/a) combined with plentiful evaporations (approximately 500 mm/a) leads to considerable precipitation (approximately 600 mm/a). The seasonal distributions of precipitation is similar to that of the annual mean, while significant differences are observed in the magnitude. The total precipitation is largest in summer, followed by spring and autumn, and lowest in winter.

Key characteristics of long-term trends in total precipitation also combines those of water vapor convergence and evaporation (Figure 11). Total precipitations exhibits an overall long-term increasing trends across the majority of the TP, with the exception of the Yarlung Zangbo Grand Canyon, which is also associated with the maximum of water vapor convergence and steepest decrease in water vapor convergence. As with the long-term trends in vertical integrated divergence of water vapor flux, the total precipitation consistently decreases around Yarlung Zangbo Grand Canyon during the entire year. This suggests the dominant role of the water vapor convergence related to atmospheric circulation dominate in the precipitation variations for this area. Generally, the locations associated with increasing precipitation vary with season. The long-term trends in summer follow that of the annual mean. In spring, precipitation increase (decrease) in south (north) of the TP, while the reverse is observed in autumn. The long-term winter trends of precipitation are generally stable. The Brahmaputra basin, inner TP and south of Qilian Mountain exhibit increases in both water vapor flux convergence and total evaporation, resulting in an obvious rise in total precipitation. The long-term trends indicate that evaporation plays a relatively important role in the increasing the precipitation in the inner TP, while water vapor convergence dominates the Brahmaputra basin and south of Qilian Mountain. For the source region of the Yangtze River, Yellow River and Lancang River is located in the central zone of eastern TP, and thus a reduction in water vapor convergence combined with an increase in evaporations dose not give rise to significant changes in total precipitations. The mechanisms about how different climate systems influences the precipitation in this region are very complex. Sun and Wang (2018, 2019) found that both Eurasian spring circulation and El Niño–Southern Oscillation (ENSO) affect the

spring precipitation, while North Atlantic Oscillation (NAO), East Asian summer monsoon and El Niño can affect summer precipitation. As this source region supplies adequate freshwater to downstream areas and feeds approximately 40% of the world's population, constant precipitation combined with an increase in evaporation will decrease the surface water storage, possibly having a dramatic effect on those relying on this water supply.

3.2.4 Discussion of Atmospheric Water Balance over the TP

In order to further investigate the long-term variation of moisture balance over the TP, the time series of annual total evaporation, precipitation and convergence of water vapor are depicted in Figure 12. Variations of annual total precipitation are in close agreement with those of the convergence of water vapor over the TP, while their long-term trends are different. Correlation coefficient between precipitation and convergence of water vapor is 0.88 and that between precipitation and evaporation is 0.28. This implies the dominance of water vapor convergence in the precipitation process across the TP, while evaporation plays an assisting role. However, evaporation makes great contributions in the increasing trend of precipitation, as both precipitation and evaporation over the TP are increasing at the rate of 0.68 mm/a and 0.69 mm/a. Convergence of water vapor showed a slightly decreasing trends, and influence by more complex changes of atmospheric circulations, such as transportation from Indian Ocean (*Xu & Gao，2019*) and cyclonic anomaly near Lake Baikal (*Zhou et al., 2019*).

Table 1 and 2 report the long-term means and trends of all the terms in Eq. (1) for the entire TP and four sub-regions in Figure 1, respectively. Values are averaged (accumulated) during the corresponding periods for the status (accumulation) parameters. The aera total values in the bottom line of Table 1 is summed by the area weighted values for the total Tibet Plateau via Eq. (6). The annual vertically integrated moisture over the TP is determined as 16.1 Gt, which is much less than the equivalent values for precipitation, evaporation and vertical integrated water vapor convergence. This result suggests that the moisture converging from surrounding regions and/or evaporating from surface generally leaves the atmosphere through precipitation, with only very small percentage of water remianing in the atmosphere. Whether it is for the entire year or each seasons, atmospheric water budget almost maintains an approximate equilibrium. The annual accumulated precipitation is determined as 2220.0 Gt, which is slightly less than the sum of the convergence of moisture (1103.6 Gt) and evaporation (1245.5 Gt). This indicates that more water vapors might left in atmosphere. Coincidently, total column water (TCW) is observed to rise steadily at the rate of 0.011 mm/a.

Checking trends of water vapor convergence in different seasons (Table 1), it only increased in summer but decreased in other three seasons. During summer, both water vapor convergence and evaporation brings about increasing in precipitation, convergence of water vapor (0.3 mm/a) contributes more than evaporation (0.18 mm/a). We can speculate that the long-term trends of water storage in the TP is increasing in summer, which is the largest atmospheric water obtain season. Although the water vapors obtained in relatively cold seasons were relative small, precipitation are usually in solid form, which is very important to surface water storage. However, water vapor transported from outsides keep decreasing in relatively cold seasons, particularly in autumn.

Generally, changes in convergence of water vapor are attributed to the changes in the atmospheric circulation, while the enhanced evaporation is a result of expansion of the lake area and the melting of glaciers over the TP. Therefore, evaporation acts as a local source for atmospheric water vapor, while the divergence of water vapor flux is linked principally to the water transported from outside of the TP. A continuous and significant decrease in water vapor convergence, the water storage of TP will be further depleted. For different sub regions over

the TP, the long-term variations of water storage show different trends (Table 2). Surface water storage at the region around Yarlung Zangbo Grand Canyon experienced tremendously lost. For the source region of the Three Rivers, water storage are also under a risk of depletion in the further as decreasing of water vapor convergence and larger increasing of evaporation than that of precipitation. For both Brahmaputra basin and inner TP, there are significant wetting tendencies because that the increases in both convergence of water vapor flux and evaporation bring about obvious increase in total precipitation. As Brahmaputra basin is much wetter than inner TP, the increasing trends of TCW in inner TP are more significant.

Figure 13 presents the monthly climatology of the precipitation, evaporation and convergence of water vapor. Divergence of water vapor flux, evaporation and precipitation exhibit a single-peak seasonal variation that is stronger in summer and weaker in winter. Precipitation overwhelms evaporation during the warmer months of the year, while the colder months exhibit the same trend but with a slightly lower difference between the two variables. This suggests that a gain in the gross surface water budget in the TP. The residuals of the water vapor balance should include the phase transformation of water vapor and the cross-tropopause mass exchange, both of which are theoretically minimal (*Tian et al., 2014*). Negative residual imply an excess of water vapor resources left in the atmosphere, with positive values indicating that more moisture is removed from atmosphere by precipitation. Thus, the monthly-accumulated residual term with small negative number can be neglected.

4 Conclusions

The Tibetan Plateau (TP), considered as the "Asian Water Tower" (*Yao et al., 2012*), acts as a “heat pump” that acquires water vapor from the surrounding oceans to the plateau region. Combined with the local evaporation, TP forms an isolated region of atmospheric humidity (*Wu et al., 2007; Xu et al., 2008*) known as the “Atmospheric Water Tower (AWT)” of the plateau. We employed ERA5 reanalysis data from 1979 to 2018 to determine a minor drying trend for the general characteristics of the AWT in southern and southeastern TP, where is the wettest region of the TP, but marked wetting trends in the northwest, northeast and surrounding zones of the TP, where are relatively dryer regions of the TP.

In order to determine whether water vapor supply can alleviate the depletion of the surface water storage caused by the melting of glaciers and the increase in runoff under rapid warming, we analyzed the long-term trends in the water vapor budget components, including water vapor transportation, evaporation and precipitation over the TP. Annual accumulated precipitation (2220.0 Gt) across the TP is almost equivalent to the sum of convergence of moisture (1103.6 Gt) and evaporation (1245.5 Gt). Despite the increase in the long-term trend in total precipitation at the rate of 0.68 mm/a, the surface water storage is not fully replenished because that the evaporation increases at the rate of 0.69 mm/a, while the net gain of water vapor transportation does not exhibit significant long-term changes. These observations are based on two independent methods: i) the integration of the water vapor flux along the boundary of the TP; and ii) the integration of the divergence of water vapor flux within the enclosed area of the TP. Note that the the largest amount of water is obtained during summer, and the trend in convergence of water vapor flux increases significantly at the rate of 0.3 mm/a, which was induced by the increasing in the inflow transportation from the western boundaries and the reduced outflow transportation in the eastern boundary. *Zhou et al.* (*2019*) reports that the occurrence of a cyclonic (an anticyclonic) anomaly near Lake Baikal reduces (increases) the water vapor over the TP, and subsequently attributes the decreasing outflow in the eastern boundary to a summer atmospheric circulation anomaly near Lake Baikal. Despit of huge changes in atmospheric water vapor balance during summer, the risk of water storage depletion are brought by other three seasons, especially the autumn.

The water vapor balance characteristic and their long-term trends vary spatially across the TP. Regions close to Yarlung Zangbo Grand Canyon, where is the major passageway of water vapor transported from southern oceans to the TP, exhibit a sharp decrease in water vapor convergence that reduces precipitation. Furthermore, the evaporation is enhanced due to the rise in temperatures and the melting of glaciers, causing a marked loss in the surface water storage in this area. In the Three Rivers Source Region, the reduced water vapor convergence outbalances the increase in evaporations such that no significant changes in total precipitations are observed. As the evaporations provide the water vapor locally while water vapor convergence transport water resources from the outside of the TP, and thus the possible depilation of the water storage in this area should be noted with caution. The Brahmaputra basin, inner TP and south of Qilian Mountain exhibit significant wetting tendencies attributed to the enhanced precipitation resulting from in both convergence of water vapor flux and evaporation.

The regional feature of water vapor balance across the TP are the result of complex interactions between atmospheric heat sources (*Yang et al., 2014*), atmospheric circulation from high latitude regions, such as cyclone near the Lake Baikal (*Zhou et al., 2019*), and/or low latitude regions, such as monsoon from the Indian Ocean (*Xu & Gao, 2019*). Meanwhile, *Liu et al.* (*2019*) found that the slow increasing of precipitation may be affected by the increasing dust aerosol transported from central Asian or Taklamakan desert. In the current study, we describe the AWT and detail the impacts of the long-term changes in the atmospheric water vapor balance on surface water storage across the TP. The results can improve our understanding on the "Asia Water Tower" in climate research and adaptation policy.

Acknowledgments

This study was supported by the Strategic Priority Research Program of the Chinese Academy of Sciences (XDA2006010301). The ERA5 data are available from https://cds.climate.copernicus.eu/

References

An, Z., Kutzbach, J. E., Prell, W. L., & Porter, S. C. (2001). Evolution of Asian monsoons and phased uplift of the Himalaya-Tibetan plateau since Late Miocene times. *Nature*, 411, 62-66, https://doi.org/10.1038/35075035.

Adler, R.F., Huffman, G.J., Chang, A., Ferraro, R., Xie, P., Janowiak, J., et al. (2003). The Version 2 Global Precipitation Climatology Project (GPCP) Monthly Precipitation Analysis (1979-Present). *J. Hydrometeor.*, 4,1147-1167.

Berrisford, P., Dee, D.P., Fielding, K., Fuentes, M., Kallberg, P., Kobayashi, S., & Uppala, S.M. (2009). The ERA-Interim Archive. *ERA Report Series*, No.1. ECMWF: Reading, UK.

Boos, W. R., & Kuang, Z. (2010). Dominant control of the South Asian monsoon by orographic insulation versus plateau heating. *Nature*, 463, 218-223, doi:10.1038/nature08707.

Chen, D.L., Xu, B.Q., Yao, T.D., Guo, Z.T., Cui, P., Chen, F.H., et al., 2015: Assessment of past, present and future environmental changes on the Tibetan Plateau. *Chin. Sci. Bull.*, 60, 3025–3035, https://doi.org/10.1360/N972014-01370. (in Chinese)

Chen, X., Massman, W. J., & Su, Z. (2019). A column canopy-air turbulent diffusion method for different canopy structures. *Journal of Geophysical Research: Atmospheres*, 124, 488– 506. https://doi.org/10.1029/2018JD028883.

Cheng, G., & Wu, T. (2007), Responses of permafrost to climate change and their environmental significance, Qinghai-Tibet Plateau, *J. Geophys. Res.*, 112, F02S03, doi:10.1029/2006JF000631. Chou, C. , & Neelin, J. D. (2004). Mechanisms of global warming impacts on regional tropical precipitation. *Journal of Climate*, 17(13), 2688-2701.

Dee, D. P., Uppala, S.M., Simmons, A.J., Berrisford, P., Poli, P., Kobayashi, S., et al. (2011). The ERA-Interim reanalysis: configuration and performance of the data assimilation system. *Quart. J. R. Meteorol. Soc.*, 137, 553–597.

Deng, H., Pepin, N. C., Liu, Q., & Chen, Y. (2018). Understanding the spatial differences in terrestrial water storage variations in the Tibetan Plateau from 2002 to 2016, *Clim. Change*, 151(3–4), 379–393, doi:10.1007/s10584-018-2325-9.

Ding, Y., & Chan, J. (2005). The east Asian summer monsoon: an overview. *Meteorol. Atmos. Phys.*, 89(1):117–142.

Duan, A., & Wu, G. (2008). Weakening trend in the atmospheric heat source over the Tibetan Plateau during recent decades. Part I: observations. *J. Clim.*, 21, 3149–3164.

Duan, A., & Wu, G. (2009). Weakening trend in the atmospheric heat source over the Tibetan Plateau during recent decades. Part II: connection with climate warming. *J. Clim.*, 22, 4197–4212.

Duan, A., & Xiao, Z. (2015). Does the climate warming hiatus exist over the Tibetan Plateau?. *Sci. Rep.*, 5, 13711. https://doi.org/10.1038/srep13711.

Duan, A., Liu, S., Zhao, Y., Gao, K., & Hu, W. (2018). Atmospheric heat source / sink dataset over the Tibetan Plateau based on satellite and routine meteorological observations. *Big Earth Data*, 00(00), 1–11. https://doi.org/10.1080/20964471.2018.1514143

Feng, L., & Zhou, T. (2012). Water vapor transport for summer precipitation over the Tibetan Plateau: Multidata set analysis, *J. Geophys. Res.*, 117, D20114, doi:10.1029/2011JD017012.

Gao, L., Gou, X., Deng, Y., Wang, Z., Gu, F., Wang, F. (2018). Increased growth of Qinghai spruce in northwestern China during the recent warming hiatus. *Agricultural and Forest Meteorology*, 260–261, 9-16.

Guo, D., & Wang, H. (2012). The significant climate warming in the northern Tibetan Plateau and its possible causes. *Int. J. Climatol*. 32, 1775–1781, http://dx.doi.org/10.1002/ joc.2388.

Harris, I., Osborn, T.J., Jones, P., Lister, D. (2020). Version 4 of the CRU TS monthly high-resolution gridded multivariate climate dataset. *Scientific Data*, 7, 109, https://doi.org/10.1038/s41597-020-0453-3

Immerzeel, W.W., van Beek, L.P.H., Bierkens, M.F.P. (2010). Climate change will affect the Asian water towers. *Science*, 328, 1382–1385

Li, D., Yang, K., Tang, W., Li, X., Zhou, X., & Guo, D. (2020). Characterizing precipitation in high altitudes of the western Tibetan plateau with a focus on major glacier areas, Int. J. Climatol., (February), doi:10.1002/joc.6509.

Li, W., Guo, W., Qiu, B., Xue, Y., Hsu, P. C., & Wei, J. (2018). Influence of Tibetan Plateau snow cover on East Asian atmospheric circulation at medium-range time scales. *Nat. Commun.*, 9(1), doi:10.1038/s41467-018-06762-5.

Li, W., Qiu, B., Guo, W., Zhu, Z., & Hsu, P. C. (2019). Intraseasonal variability of Tibetan Plateau snow cover, Int. J. Climatol., (November), doi:10.1002/joc.6407.

Lin, C., Yang, K., Qin, J., & Fu, R. (2013). Observed Coherent Trends of Surface and Upper-Air Wind Speed over China since 1960. *J. Climate*, 26, 2891–2903, https://doi.org/10.1175/JCLI-D-12-00093.1.

Liu, Y., Zhu, Q., Huang, J., Hua, S., & Jia, R. (2019). Impact of dust-polluted convective clouds over the Tibetan Plateau on downstream precipitation. *Atmos. Environ.*, 209, 67-77. doi: 10.1016/j.atmosenv.2019.04.001.

Liu, X., & Chen, B. (2000). Climatic warming in the Tibetan Plateau during recent decades. *Int. J. Climatol.*, 20, 1729–1742.

Lu, C., Yu, G., & Xie, G. (2005). Tibetan Plateau serves as a water tower. *IEEE Trans. Geosci. Remote Sens.*, 5, 3120– 3123.

Luo,X., & Xu, J. (2019). Estimate of atmospheric heat source over Tibetan Plateau and its uncertainties. *Climate Change Research*, 15(1): 33-40.(in Chinese)

Lutz, A. F., Immerzeel, W. W., Shrestha, A. B., & Bierkens, M. F. P. (2014). Consistent increase in High Asia's runoff due to increasing glacier melt and precipitation, *Nat. Clim. Chang.*, 4(7), 587–592, doi:10.1038/nclimate2237.

Ma, Y., Ma, W., Zhong, L., Hu, Z., Li, M., Zhu, Z., Han, C., Wang, B., & Liu, X. (2017). Monitoring and Modeling the Tibetan Plateau's climate system and its impact on East Asia, Sci. Rep., 7, 1–6, doi:10.1038/srep44574.

Maussion, F., Scherer, D., Mölg, T., Collier, E., Curio, J., & Finkelnburg, R. (2014). Precipitation Seasonality and Variability over the Tibetan Plateau as Resolved by the High Asia Reanalysis. *J. Climate*, 27, 1910–1927, doi:10.1175/JCLI-D-13-00282.1.

Molnar, P., England, P., & Martinod, J. (1993). Mantle dynamics, uplift of the Tibetan Plateau, and the Indian Monsoon, *Rev. Geophys.*, 31(4), 357-396, doi:10.1029/93RG02030.

Moore, G.W.K. (2012). Surface pressure record of Tibetan Plateau warming since the 1870s. *Q. J. R. Meteorol. Soc.*, 138, 1999–2008.

Sugimoto, S., Ueno, K., Sha, W. (2008). Transportation of Water Vapor into the Tibetan Plateau in the Case of a Passing Synoptic-Scale Trough. *Journal of the Meteorological Society of Japan*, 86(6):935-949.

Sun, B., & Wang, H. (2018). Interannual variation of the spring and summer precipitation over the three river source region in China and the associated regimes. *Journal of Climate*, 31(18): 7441-7457.

Sun, B., & Wang, H. (2019). Enhanced connections between summer precipitation over the Three-River-Source region of China and the global climate system. *Climate Dynamics*, 52(5-6): 3471-3488.

Tian, H., Tian, W., Luo, J., Zhang, J., & Zhang, M. (2017). Climatology of cross-tropopause mass exchange over the Tibetan Plateau and its surroundings. *Int. J. Climatol.*, 37: 3999-4014, doi:10.1002/joc.4970

Ueno, K., Toyotsu, K., Bertolani, L., & Tartari, G. (2008). Stepwise onset of monsoon weather observed in the Nepal Himalayas. *Mon. Weather Rev.*, 136, 2507– 2522.

Wan, W., Long, D., Hong, Y., Ma, Y., Yuan, Y., Xiao, P., et al. (2016). A lake data set for the Tibetan Plateau from the 1960s, 2005, and 2014. *Sci. Data*, 3:160039 doi: 10.1038/sdata.2016.39

Wan, B., Gao, Z., Chen, F., & Lu, C. (2017). Impact of Tibetan Plateau Surface Heating on Persistent Extreme Precipitation Events in Southeastern China. *Monthly Weather Review*, 145, 3485–3505.

Wang, Y., Xu, X., Lupo, A. R., Li, P., & Yin, Z. (2011). The remote effect of the Tibetan Plateau on downstream flow in early summer. *J. Geophys. Res.*,116, D19108, doi:10.1029/2011JD015979.

Wang, Y., Yang, K., Pan, Z., Qin, J., Chen, D., Lin, C., et al. (2017). Evaluation of precipitable water vapor from four satellite products and four reanalysis datasets against GPS measurements on the Southern Tibetan Plateau. *J. Clim.*, 30(15), 5699–5713, doi:10.1175/JCLI-D-16-0630.1.

Wu, G., Liu, Y., He, B., Bao, Q., Duan, A., Jin, F. F. (2012a). Thermal controls on the Asian summer monsoon. *Sci. Rep.*, 2, 4, https://doi.org/10.1038/ srep00404.

Wu, G. X., Liu, Y. M., Dong, B. W., Liang, X. Y., Duan, A. M., Bao, Q., & Yu, J. J. (2012b). Revisiting Asian Monsoon Formation and Change Associated with Tibetan Plateau Forcing: I. Formation. *Clim. Dyn.*, 39(5), 1169-1181, doi:10.1007/s00382-012-1334-z.

Wu, G. X., Liu, Y. M., Wang, T. M., Wan, R. J., Liu, X., Li, W. P., et al. (2007). The influence of mechanical and thermal forcing by the Tibetan Plateau on Asian climate, *J. Hydro. Meteor. Spec. Sect.*, 8, 770-789, doi:10.1175/JHM609.1.

Wu, G. X., & Zhang, Y. S. (1998). Tibetan Plateau Forcing and the Timing of the Monsoon Onset over South Asia and the South China Sea. *Monthly Weather Review*, 126(4):913-927.

Xu, X., Zhou, M., Chen, J., Bian, L., Zhang, G., Liu, H., et al. (2002). A comprehensive physical pattern of land-air dynamic and thermal structure on the Qinghai-Xizang Plateau, *Science in China Series D: Earth Sciences*, 45(7), 18–24.

Xu, X., Lu, C., Shi, X., & Gao, S. (2008a). World water tower: An atmospheric perspective. *Geophys. Res. Lett.*, 35(20), 525-530, doi:10.1029/2008GL035867.

Xu, X. D., Shi, X. Y., Wang, Y. Q., Peng, S. Q., & Shi, X. H. (2008b). Data analysis and numerical simulation of moisture source and transport associated with summer precipitation in the Yangtze River Valley over China. *Meteorol. Atmos. Phys.*, 100, 217-231, doi:10.1007/s00703-008-0305-8.

Xu, Y., & Gao, Y. (2019). Quantification of evaporative sources of precipitation and its changes in the Southeastern Tibetan Plateau and Middle Yangtze River Basin. *Atmosphere*, 10(8). https://doi.org/10.3390/atmos10080428.

Yang, K., Guo, X., & Wu, B. (2011a). Recent trends in surface sensible heat flux on the Tibetan Plateau. *Science in China Series D: Earth Sciences*, 54, 19–28.

Yang, K., Guo, X., He, J., Qin, J., & Koike, T. (2011b). On the climatology and trend of the atmo- spheric heat source over the Tibetan Plateau: an experiments-supported revisit. *J. Clim.*, 24, 1525–1541.

Yang, K., Wu, H., Qin, J., Lin, C., Tang, W., & Chen, Y. (2014). Recent climate changes over the Tibetan Plateau and their impacts on energy and water cycle: A review. *Glob. Planet. Change*, 112, 79–91, doi:10.1016/j.gloplacha.2013.12.001.

Yao T., Thompson, L., Yang, W., Yu, W., Gao, Y., Guo, X., et al. (2012). Different glacier status with atmospheric circulations in Tibetan Plateau and surroundings. *Nat. Clim. Change*, 2: 663–667.

Yao, T. (2019). Tackling on environmental changes in Tibetan Plateau with focus on water, ecosystem and adaptation. *Science Bulletin*, 64: 417

Yin, Y., Wu, S., Zhao, D., Zheng, D., & Pan, T. (2013). Modeled effects of climate change on actual evapotranspiration in different eco-geographical regions in the Tibetan Plateau. *J. Geogr. Sci.*, 23, 195–207.

Zhang, D., Huang, J., Guan, X., Chen, B., & Zhang, L. (2013). Long-term trends of precipitable water and precipitation over the Tibetan Plateau derived from satellite and surface measurements. *Journal of Quantitative Spectroscopy & Radiative Transfer*, 122:64-71.

Zhang, Y., Liu, C., Tang, Y., & Yang, Y. (2007). Trends in pan evaporation and reference and actual evapotranspiration across the Tibetan Plateau, *J. Geophys. Res. Atmos.*, 112(12), 1–12, doi:10.1029/2006JD008161.

Zhang, C., Liu, F., & Shen, Y. (2018), Attribution analysis of changing pan evaporation in the Qinghai–Tibetan Plateau, China. *Int. J. Climatol*, 38, e1032-e1043, doi:10.1002/joc.5431

Zhao, Y., & Zhou, T. (2019). Asian water tower evinced in total column water vapor: a comparison among multiple satellite and reanalysis data sets. *Clim. Dyn.*, 54, 231-245, doi:10.1007/s00382-019-04999-4.

Zhou, C., Zhao, P., & Chen, J. (2019). The interdecadal change of summer water vapor over the Tibetan Plateau and associated mechanisms. *J. Clim.*, 32, 4103–4119, doi:10.1175/JCLI-D-18-0364.1.

Zhu, Y.X., Ding, Y.H., & Xu, H.G. (2008). Decadal relationship between atmospheric heat source of winter and spring snow over Tibetan Plateau and rainfall in East China. *Journal of Meteorological Research*, 65, 946–958.

Zhu, L., Xie, M., & Wu, Y. (2010). Quantitative analysis of lake area variations and the influence factors from 1971 to 2004 in the Nam Co basin of the Tibetan Plateau. *Chinese Science Bulletin*, 55, 1294–1303.

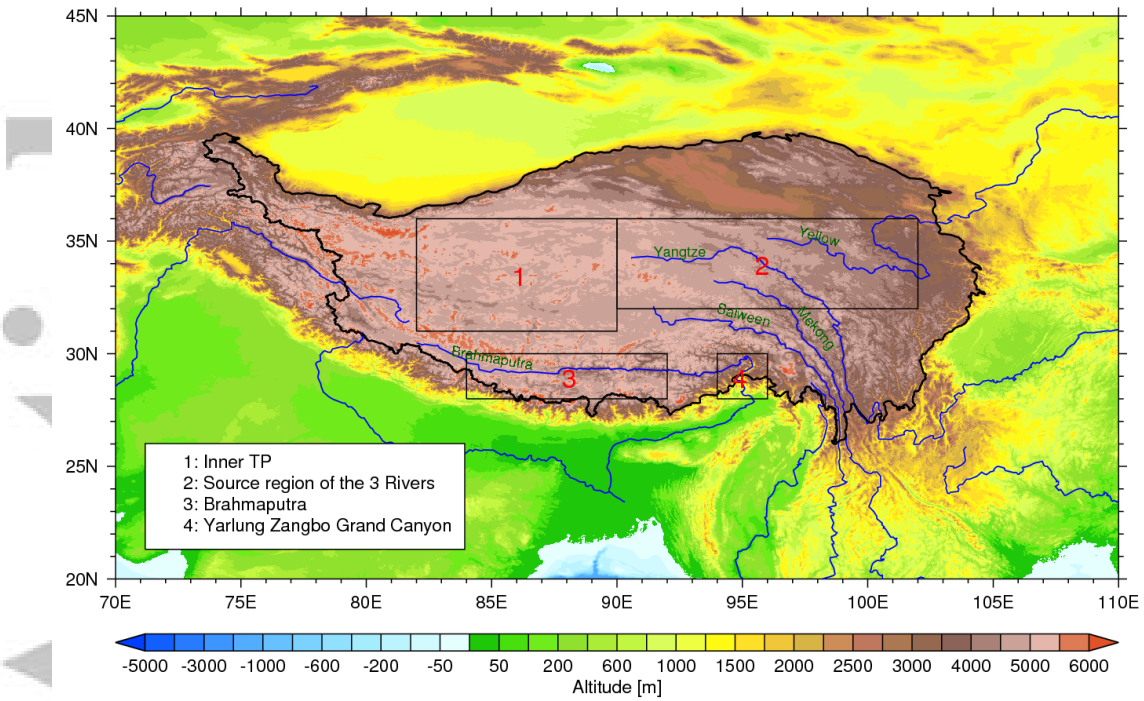

Figure 1. Topography of the TP and four sub-regions.

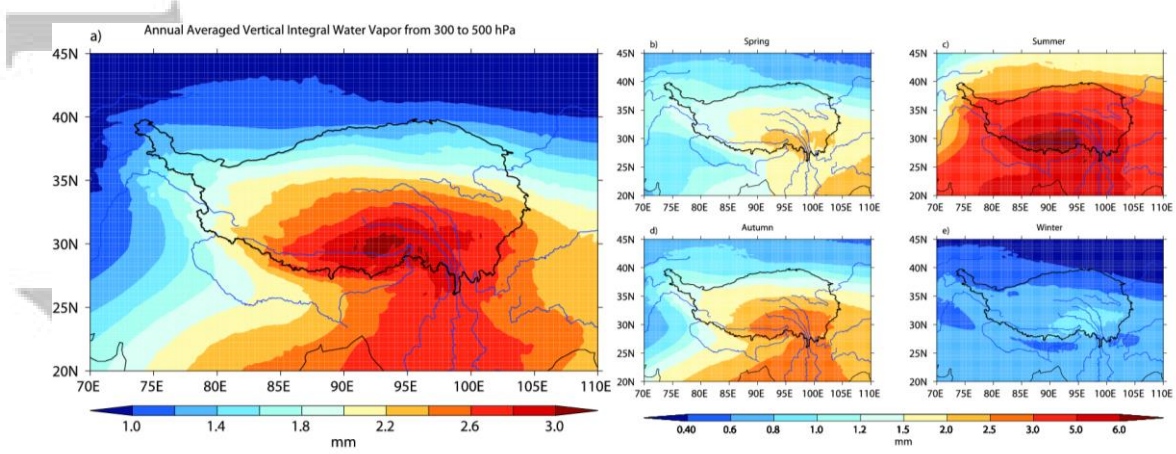

Figure 2. Horizontal distribution of 40-year (1979-2018) averaged water vapor content vertically integrated from 500 hPa to 300 hPa over the TP. (a) Annual, (b) spring, (c) summer, (d) autumn, and (e) winter values. The thin black thick line denotes the outline of the TP.

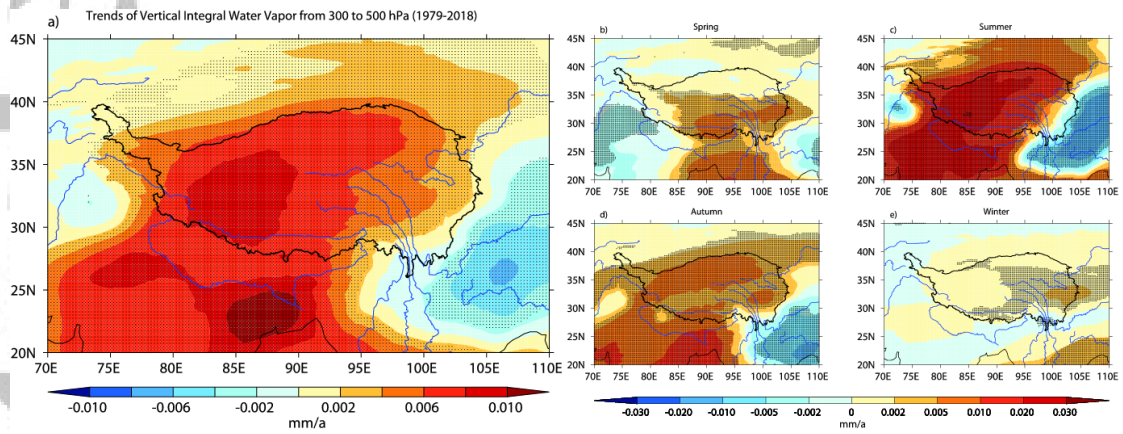

Figure 3. Long-term (1979-2018) horizontal distribution trends of 500-300 hPa vertical integral water vapor content over the TP. (a) Annual, (b) spring, (c) summer, (d) autumn, and (e) winter values. Black dot denotes the trends in the corresponding grid at the 95% confidence level..

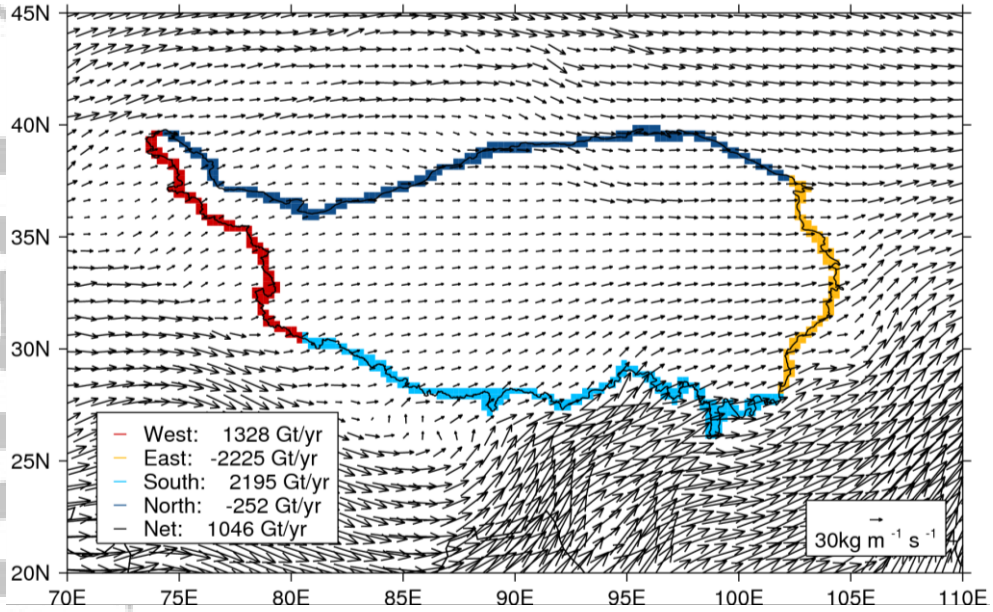

Figure 4. Vertical integral of water vapourvapor flux from ERA5 (1979-2018) over the Qinghai-Tibet Plateau, whose western, southern, eastern and northern boundaries are denoted in red, light blue, yellow and navy blue, respectively.

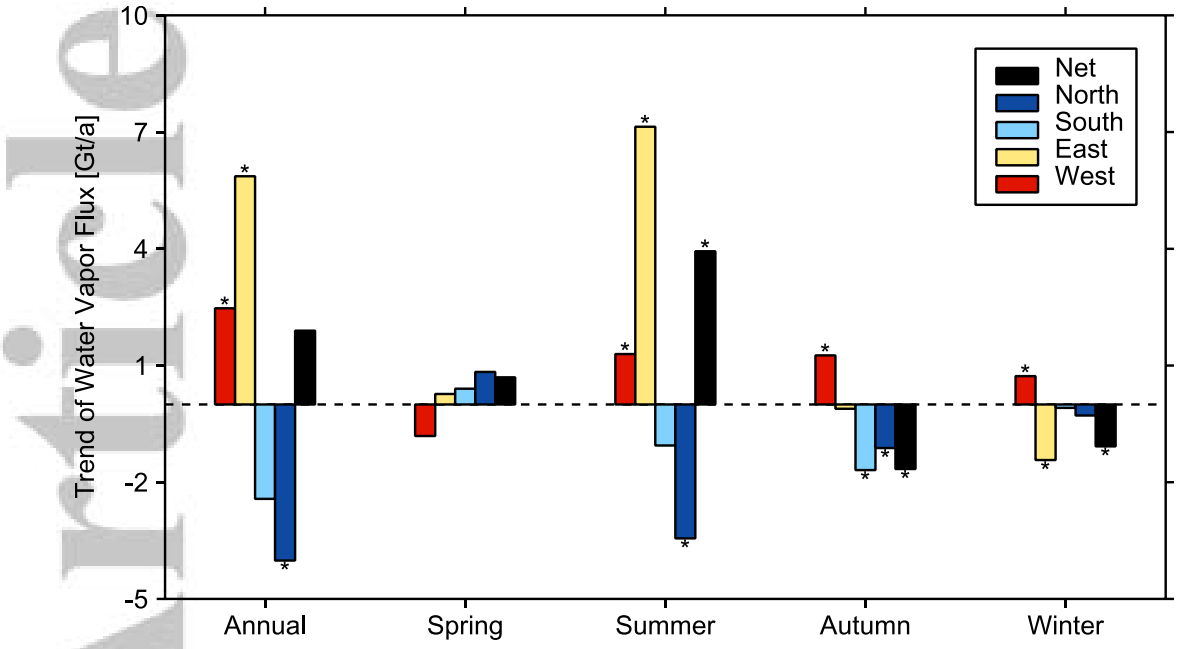

Figure 5. Seasonal and annual long-term (1979-2018) net water vapor flux for the north (deep blue), south (light blue), east (yellow), west boundary (red) of the Qinghai-Tibet Plateau and net flux (black). * denotes a significant trend is significant at the 0.05 probability level.

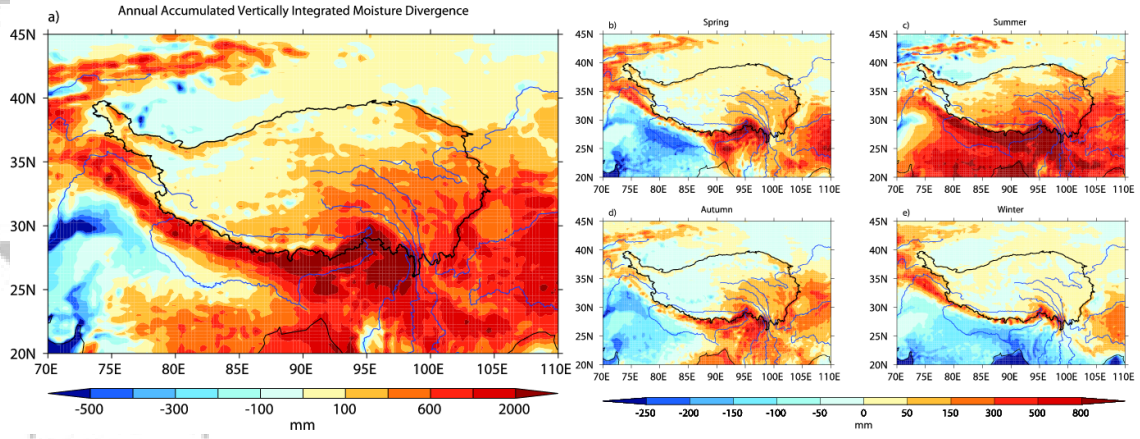

Figure 6. Horizontal distribution of 40-year (1979-2018) averaged vertical integrated divergence of water vapor flux over the TP. (a) Annual, (b) spring, (c) summer, (d) autumn, and (e) winter values.

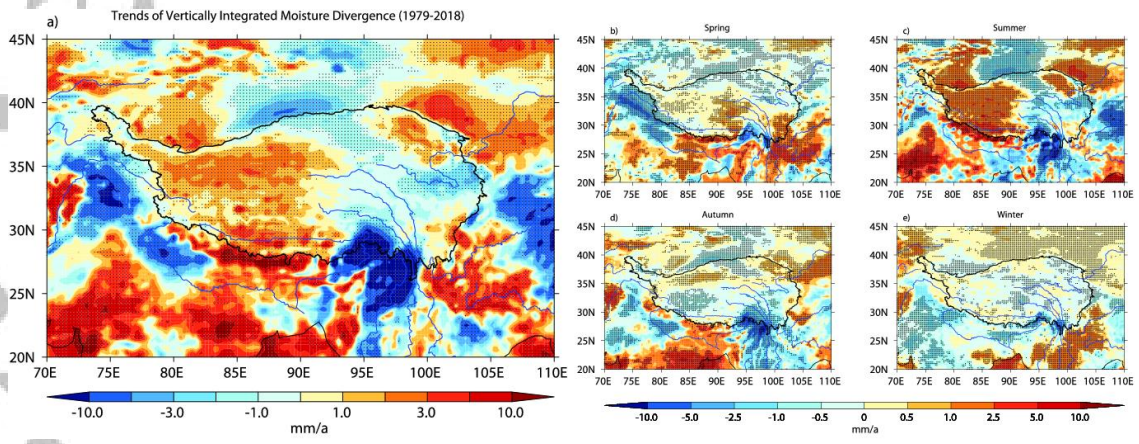

Figure 7. Horizontal distribution of long-term (1979-2018) trends in the vertical integrated divergence of water vapor fluxes over the TP. (a) Annual, (b) spring, (c) summer, (d) autumn, and (e) winter values.

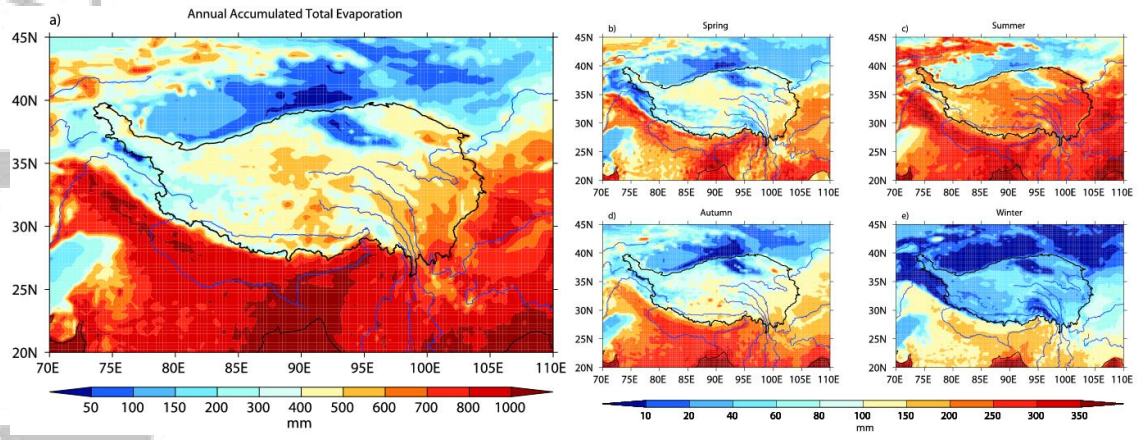

Figure 8. Horizontal distribution of 40-year (1979-2018) averaged evaporation over the TP. (a) Annual, (b) spring, (c) summer, (d) autumn, and (e) winter values.

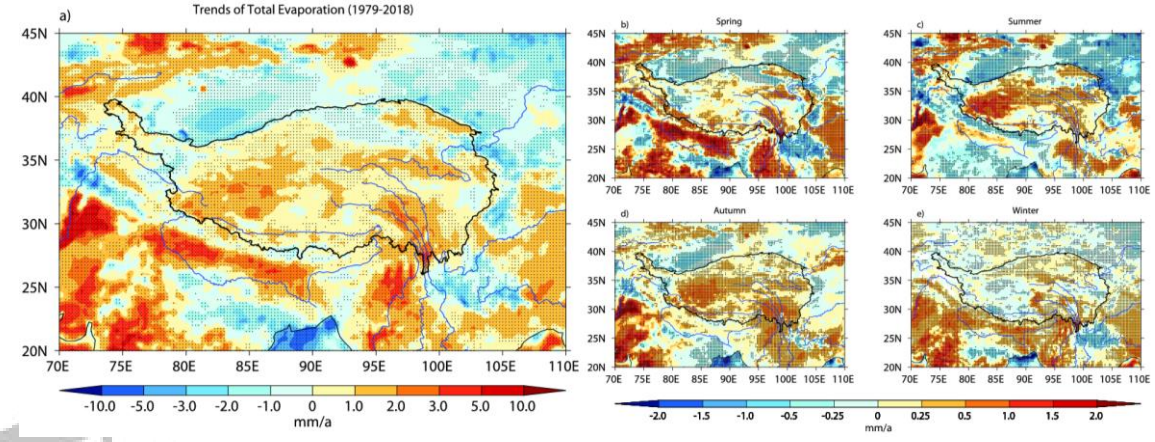

Figure 9. Horizontal distribution of long-term (1979-2018) trends in evaporation over the TP. (a) Annual, (b) spring, (c) summer, (d) autumn, and (e) winter values.

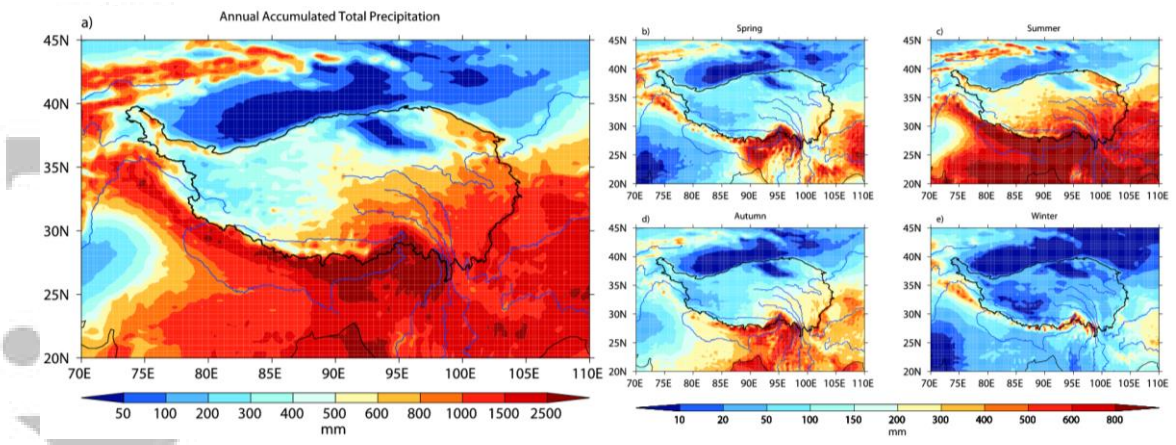

Figure 10. Horizontal distribution of 40-year (1979-2018) averaged total precipitation over the TP. (a) Annual, (b) spring, (c) summer, (d) autumn, and (e) winter values.

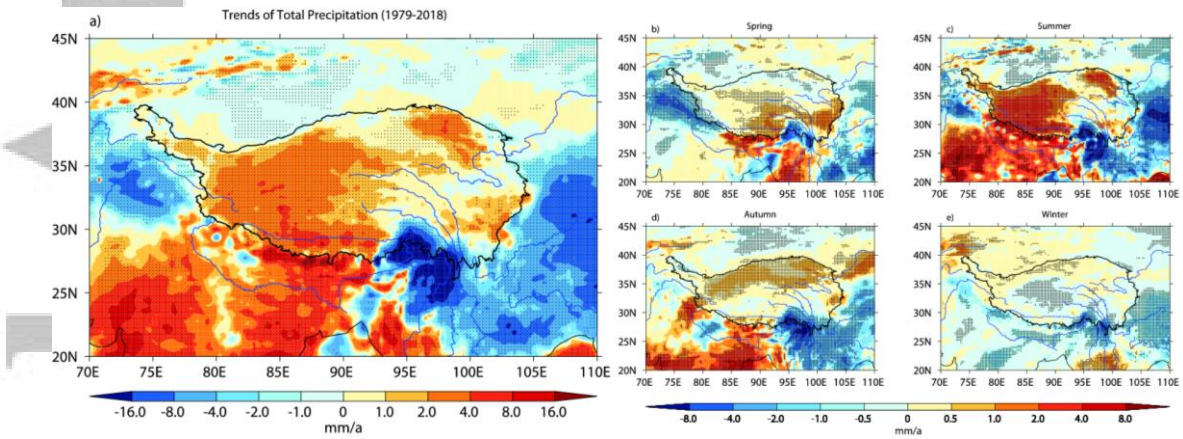

Figure 11. Horizontal distribution of long-term (1979-2018) trends in total precipitation over the TP. (a) Annual, (b) spring, (c) summer, (d) autumn, and (e) winter values.

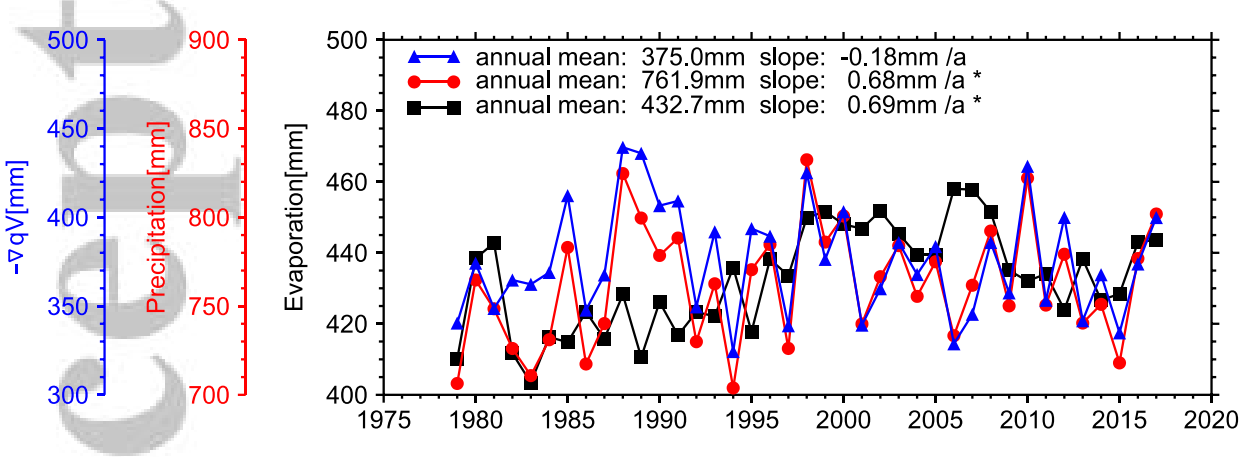

Figure 12. Time series (1979-2018) of annual vertical integrated divergence of water vapor flux (blue), total precipitation (red) and total evaporation (black) over the TP.

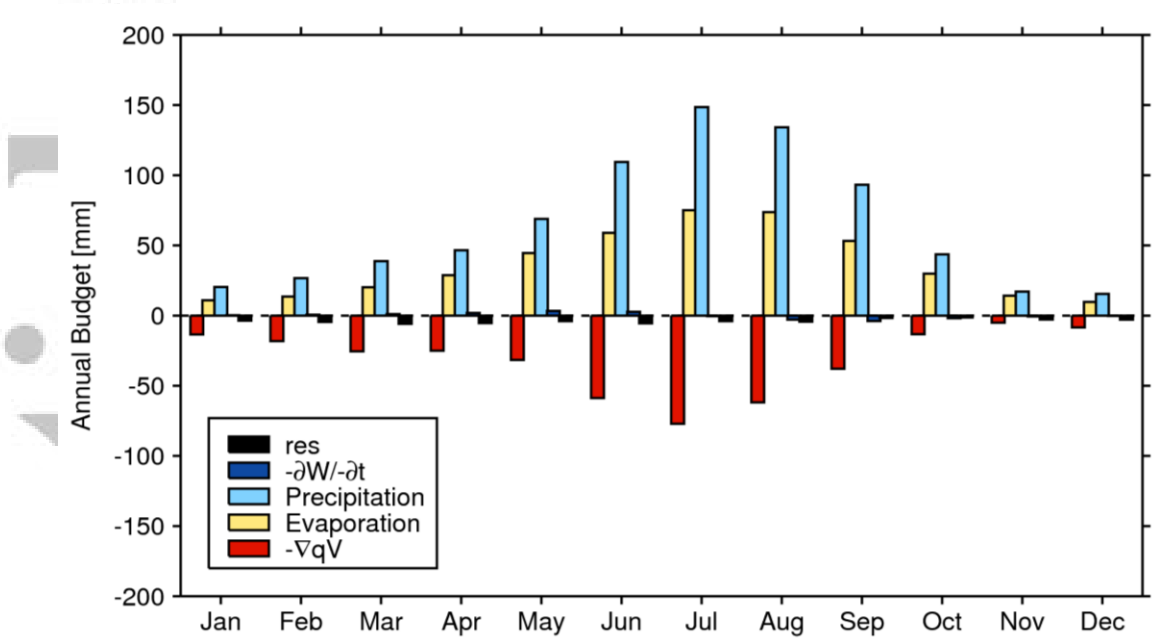

Figure 13. Climatology (1979-2018) of annual variation of $\frac{\partial w}{\partial t}$ (deep blue), precipitation (light blue), evaporation (yellow) and vertical integrated divergence of water vapor flux (red) and residual (black).

Table 1. Atmospheric water budgets over the TP. All terms are described in Eq. (1).

	TCW Mean/Trend	**∂W** Mean/Trend	**$-\nabla(q\vec{V})$** Mean/Trend	**E** Mean/Trend	**P** Mean/Trend
Property	Status	Accumulated	Accumulated	Accumulated	Accumulated
Spring [mm]/[mm/a]	3.8/0.00	6.3/0.02	82.4/-0.04	93.5/0.14*	154.6/0.04
Summer [mm]/[mm/a]	10.4/0.03	-0.6/0.00	196.4/0.30	207.6/0.18*	390.7/0.76*
Autumn [mm]/[mm/a]	4.9/0.01	-6.3/-0.03	55.9/-0.31*	97.2/0.28*	153.7/-0.01
Winter [mm]/[mm/a]	1.8/0.00	0.7/0.00	40.2/-0.12	34.3/0.08*	62.9/-0.12
Annual [mm]/[mm/a]	5.2/0.01	0.0/0.00	375.0/-0.18	432.7/0.69*	761.9/0.68*
Annual of Area total [Gt]/[Gt/a]	16.1/0.03	0.0/0.00	1103.6/-0.54	1245.5/1.99*	2220.0/1.89*

Note. * denotes significant trend at the 95% confident level.

Table 2. Annual atmospheric water budgets over four sub-regions of the TP. Regions are displayed in Figure 1.

	TCW Mean/Trend [mm]/[mm/a]	**$-\nabla(q\vec{V})$** Mean/Trend [mm]/[mm/a]	**E** Mean/Trend [mm]/[mm/a]	**P** Mean/Trend [mm]/[mm/a]
Inner TP	3.43/0.013*	49.26/1.707*	425.51/1.217*	409.60/2.894*
Three Rivers Source Region	4.797/0.010*	302.65/-0.598	475.5/0.898*	698.92/0.862*
Brahmaputra Basin	5.55/0.014*	449.49/2.72	346.90/0.191	911.78/3.924*
Yarlung Zangbo Grand Canyon	17.22/0.008	3428.35/-22.292*	606.60/0.597*	3939.35/-24.815*

Note. * denotes significant trend at the 95% confident level.